



HAL
open science

Nano-engineered prepreg manufacturing: control of capillary rise of resin into VACNTs' forests

Anh Tuan Le, Quentin Govignon, Samuel Rivallant, Thierry Cutard

► To cite this version:

Anh Tuan Le, Quentin Govignon, Samuel Rivallant, Thierry Cutard. Nano-engineered prepreg manufacturing: control of capillary rise of resin into VACNTs' forests. *Carbon Letters*, 2023, 33, pp.1019-1025. 10.1007/s42823-023-00495-2 . hal-04038875

HAL Id: hal-04038875

<https://imt-mines-albi.hal.science/hal-04038875>

Submitted on 22 Mar 2023

HAL is a multi-disciplinary open access archive for the deposit and dissemination of scientific research documents, whether they are published or not. The documents may come from teaching and research institutions in France or abroad, or from public or private research centers.

L'archive ouverte pluridisciplinaire **HAL**, est destinée au dépôt et à la diffusion de documents scientifiques de niveau recherche, publiés ou non, émanant des établissements d'enseignement et de recherche français ou étrangers, des laboratoires publics ou privés.

Nano-engineered prepreg manufacturing: control of capillary rise of resin into VACNTs' forests

Anh Tuan Le^{1,2}  · Quentin Govignon¹  · Samuel Rivallant²  · Thierry Cutard¹ 

Abstract

The incorporation of vertically aligned carbon nanotubes (VACNTs) between composites plies has been said to enhance the through-thickness strength, and it can also decrease the risk of interply delamination and reduce crack initiation. Thanks to these high mechanical performances, nano-engineered hybrid composites are seen as promising for highly demanding structural reinforcement applications. This paper is part of a study that focuses specifically on the methodology for trans-ferring VACNTs onto a prepreg surface while maintaining their initial vertically aligned morphology. The chosen method involved bonding the VACNTs' forest through capillary impregnation of the forest by the prepreg's resin. Key parameters for an effective transfer and to achieve a partial capillary rise of the resin into the VACNTs will be discussed here.

1 Introduction

Composite materials play an increasingly important role in a wide range of applications, including aerospace, due to their high mechanical properties as well as their lightness [1–4]. However, delamination during fatigue or impact loading is one of the major drawbacks of such materials [5–7].

Since the turn of the twenty-first century, the discovery and scientific investigation of nanomaterials have been increasingly prevalent across a wide range of applications, including chemistry [8–10], biology [11], and environment [12].

In this context, the introduction of nanoconstituents has been proposed to reinforce composite structures throughout their thickness [13]. For example, several publications demonstrate that the presence of carbon nanotubes (CNTs) in matrix improves both the mechanical [14–16], electrical [17, 18], and thermal [19–22] properties of composites. Improvements of in-plane and interlaminar properties of the composites with adjunction of VACNTs between composite plies are also observed [23–25].

As far as we are concerned, literature on hybrid composite VACNTs—prepreg manufacturing details are limited so far. In the previous works, Garcia, Wardle et al. [26, 27] described the VACNTs' transfer process from their initial rigid Si substrate onto prepreg bonding on a cylinder. The VACNTs' forests separate from Si wafer and then bond on prepreg surface by capillary force. In consequence, the nano-transferred prepreg surface is limited by cylinder's lateral surface.

Furthermore, Garcia et al. [28] suggest nano-engineered composites based on the capillarity principle, where the liquid impregnated to VACNTs ends by capillary rise. The authors have not fully given the relationship between resin capillary rise height and process parameters (temperature, pressure, etc.). Beard et al. [29] estimated capillary rise height versus liquid viscosity. The authors used VACNTs with heights ranging from 400 to 700 μm , an electrically conductive chromium-complex dye additive was blended

✉ Anh Tuan Le
anh_tuan.le@mines-albi.fr; leanhtuan@outlook.fr

Quentin Govignon
quentin.govignon@mines-albi.fr

Samuel Rivallant
samuel.rivallant@isae-supaero.fr

Thierry Cutard
thierry.cutard@mines-albi.fr

¹ Institut Clément ADER (ICA), Université de Toulouse, CNRS, IMT Mines Albi, INSA, ISAE-SUPAERO, UPS, Campus Jarlard, 81013 Albi, France

² Institut Clément ADER (ICA), Université de Toulouse, CNRS, IMT Mines Albi, INSA, ISAE-SUPAERO, UPS, Avenue Edouard BELIN, 31400 Toulouse, France

with low viscosity resin to simplify the resin capillary rise height. According to Sojoudi et al. [30], one of the major risks of this process is VACNTs' coalescence due to high resin-VACNTs' surface tension during capillary rise, which degrades the VACNTs' initial morphology.

The aforementioned works give an idea to impregnate resin into VACNTs' forest by resin capillary rise. However, the determination of capillary rise height over time and the consideration of substrate roughness have not fully been reported. The main objective in this work consists of observing the resin impregnation into VACNTs' forest by capillary rise while taking into consideration material properties, such as dense VACNTs' forest, limited VACNTs height, highly viscous resin without electrically conductive additive, and prepreg roughness, which could make the impregnation process and the resin capillary rise height determination difficult. These criteria allow us to manufacture a semi-product which helps to study nano-engineered composites manufacturing afterwards. Hence, this paper deals with manufacturing process which transfers VACNTs' forests from Al substrate to prepreg surface. Process parameter intervals are suggested to partially impregnate resin into VACNTs' forests. SEM images allow to observe VACNTs' morphology after impregnation process as well as capillary rise height.

To achieve this objective, capillary rise of resin from prepreg into VACNTs' forests could help maintain nanotubes' morphology and partial capillary height is targeted to reach the optimal transfer: half rise from inferior prepreg ply and another half rise from superior prepreg ply fill completely resin into VACNTs' forests. In fact, the resin impregnated at VACNTs ends forms a bond to keep VACNTs' forests on prepreg surface. The partial capillary rise also represents impregnation control, which is useful to avoid coalescence phenomenon in VACNTs' forests due to surface tension. Moreover, VACNTs ends not yet

impregnated with resin could be lightly pressed to create reinforced contact between VACNTs and prepreg surface.

2 Experimental

2.1 Materials

The prepreg reference used for the experiment is Hexply® M18/32%/UD116/M55J/300 mm, which is made of unidirectional M55J carbon fibre and M18 thermosetting epoxy resin. The average filament diameter of M55J is 5 µm (SEM images in Fig. 1), and the viscosity of M18 at 60 °C and 80 °C is 280 Pa.s and 60 Pa.s, respectively.

Multi-walled carbon nanotubes' forests are synthesised by Continuous Chemical Vapour Deposition (CCVD) method [31, 32], by our industrial partner NAWA Technologies, on a 50 µm-thick aluminium (Al) substrate. The density of VACNTs (D_{VACNTs}) is about 2.10^{11} tubes/cm², with an average height of 30 µm (a higher value of height increases spacing between two prepreg plies and it is likely to make delamination), and VACNTs have an average diameter (d_{VACNTs}) of 8 nm. The volume fraction of VACNTs can therefore be estimated at approximately 10% following Eq. (1):

$$\psi_{VACNTs} = \pi \left(\frac{d_{VACNTs}}{2} \right)^2 D_{VACNTs}, \quad (1)$$

with ψ_{VACNTs} volume fraction of VACNTs, d_{VACNTs} their average diameter, and D_{CNTs} their density.

Assuming that the interior of the VACNTs cannot be filled with resin, the amount of resin necessary to impregnate the VACNTs' forests can be estimated to ~27 ml/m².

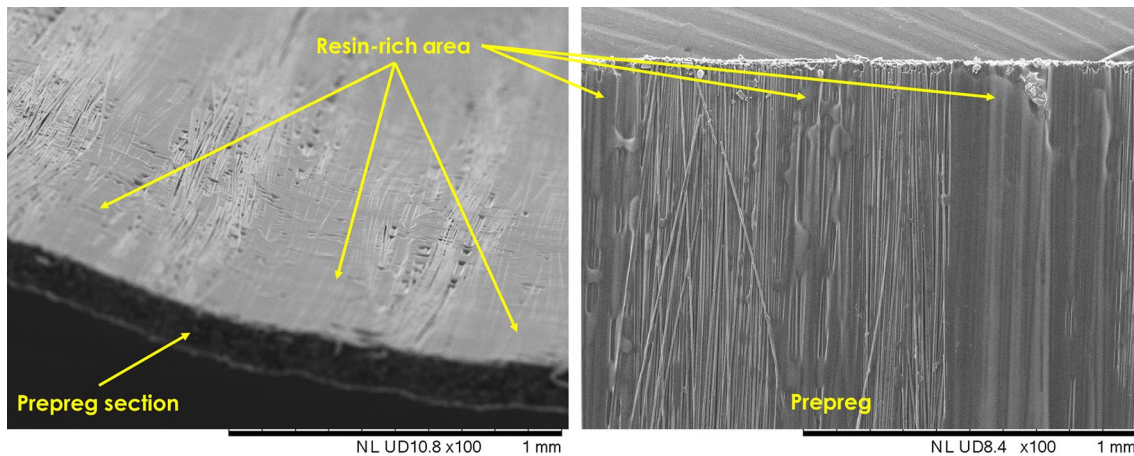


Fig. 1 SEM images showing prepreg roughness due to 5 µm elementary filament and resin distribution before the process

2.2 Impregnation and transfer process

To transfer the VACNTs from Al substrate to the prepreg surface, the controlled impregnation of resin in the VACNTs' forests by capillary rise is carried out. Partially impregnating the resin at only one end of the VACNTs is privileged. Indeed, prepreg's resin impregnated in VACNTs' forests gives high bonding and the VACNTs can remain on prepreg surface after substrate removal. Controlling resin impregnation can avoid VACNTs-resin coalescence and make it possible to preserve VACNTs' morphology after the impregnation process.

Figure 2 illustrates the impregnation process by resin capillary rise, where the viscosity of the resin is adjusted by controlling the temperature and the capillary rise height is controlled by the contact time. Pressure is also applied on the transfer zone to ensure good contact between the VACNTs and the prepreg surface. After a given impregnation time, the platens are separated, and the sample is removed and cooled to freeze the resin. The growth substrate can then be peeled off. To enable precise control of the temperature and pressure applied on a small sample, a Nanotest™ Thermal Interface Material Analyser (TIMA) [33], which is

designed for thermo-mechanical characterisation of thermal interface materials, was used.

Table 1 summarises the ranges of selected parameters during the impregnation process and provides a priori justification for the choices.

2.3 Results and discussion

2.4 Capillary rise

The capillary impregnation of the VACNTs was determined by SEM observations of the samples, as illustrated in Fig. 3. While the presence of resin cannot be directly observed and no chemical contrast appears, several clues can help determine the resin level in the VACNTs' forests. A slight coalescence of the carbon nanotubes caused by the capillary impregnation can be observed in the impregnated areas. While the dry nanotubes appear slightly frizzy, they appear much straighter in the impregnated zone due to VACNTs-resin surface tension. At a larger scale, a variation of the grey levels on the SEM images can also give hints of the resin front position.

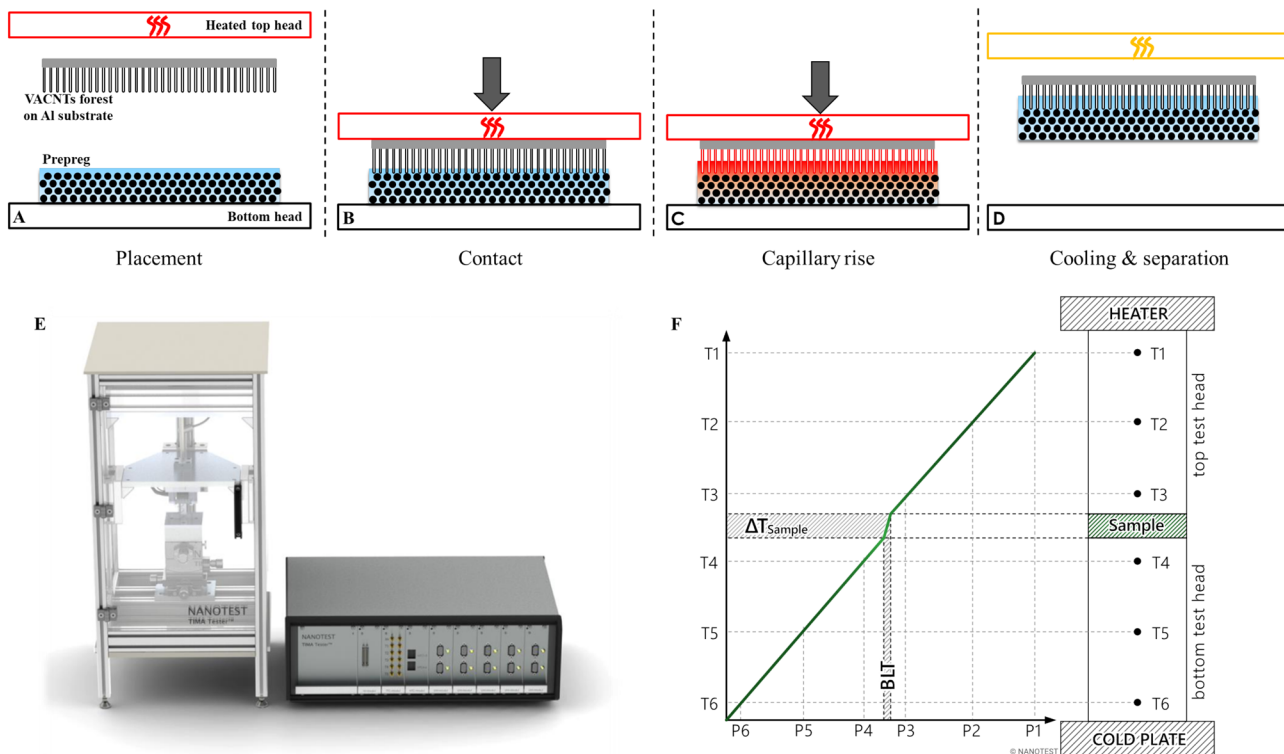


Fig. 2 Four-step impregnation process. **a** Placement of materials and pre-heating of the top head; **b** contact between heated top head, Al substrate, VACNTs, prepreg, and ambient bottom head; **c** capillary rise of resin in the VACNTs; **d** end of process by moving the two

heads apart and removing the sample; **e** picture of the Nanotest™ TIMA apparatus; **f** schematic of the determination of the sample temperature (figs. **e** and **f** courtesy of Nanotest [33])

Table 1 Three process parameters and their ranges

Impregnation parameters	Below inferior threshold	Inferior threshold	Superior threshold	Above superior threshold
Temperature	High resin viscosity, difficult impregnation of the VACNTs' forests	60 °C (Viscosity of the resin ~ 280 Pa.s)	80 °C (Viscosity of the resin ~ 60 Pa.s)	Low resin viscosity leading to fast capillary rise, resin impregnation uncontrolled
Contact time (step of 5 min)	Lack of repeatability due to handling variability and transient phase of heating, loading, and unloading	5 min	20 min	Strong possibility of full capillary rise
Pressure	Higher risk of uneven contact between VACNTs' forests and prepreg	20 kPa	200 kPa	High risk of VACNTs' buckling

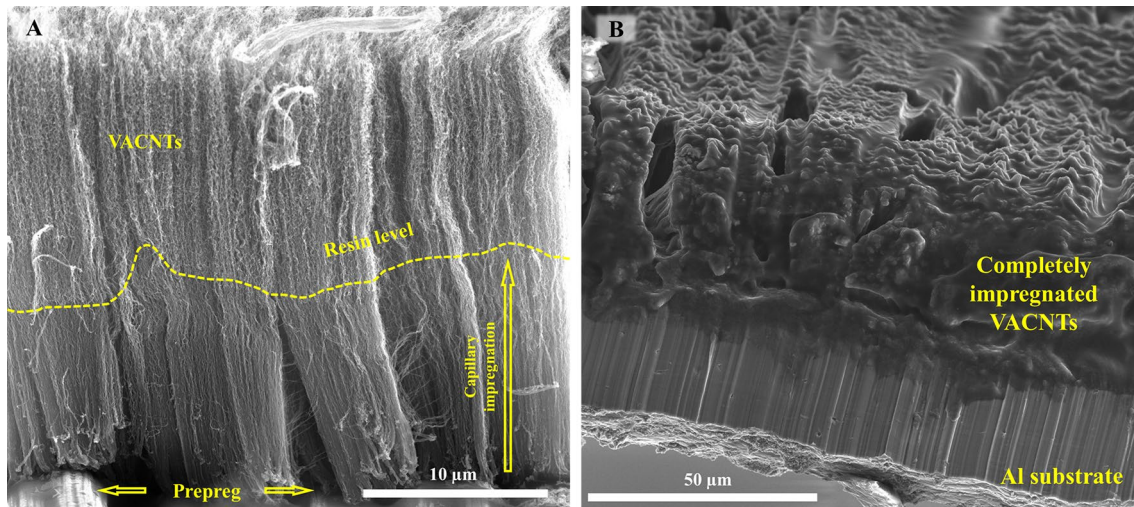


Fig. 3 SEM images illustrating **a** vertically aligned morphology of carbon nanotubes on prepreg surface and resin partial capillary rise at the bottom of these nanotubes; **b** total resin impregnation in VACNTs, and sample process parameters: 80 °C–5 min—200 kPa

The level of capillary rise displays a significant variability within a sample. This can be partly explained by local variation in the VACNTs' density caused by whether growth condition or impregnation induced coalescence, as well as the variation in the contact between the VACNTs' forests and the prepreg, and the local resin availability at the surface of the prepreg.

Figure 3a shows VACNTs' forests transferred onto prepreg surface and resin partial capillary rise at the bottom of VACNTs, with the resin level highlighted by a yellow dashed line. Figure 3b illustrates total resin impregnation into VACNTs' forests, where the resin is visible all the way to the aluminium substrate, and the VACNTs' forests remained on Al growth substrate. This demonstrates that total resin impregnation is not favourable to the transfer process as the resin might adhere to the growth substrate. For each impregnated sample, the capillary rise of the resin in the VACNTs' forests is measured at approximately ten locations to determine an average capillary impregnation level.

Capillary impregnation is most commonly described using Lucas–Washburn (LW) model [34]. For non-circular capillaries, with varying pore sizes and introducing a level of tortuosity in the capillaries, the LW equation can be expressed as [35, 36]

$$h^2 = \frac{F_{geo} \cdot D_h \cdot \gamma \cdot \cos\theta}{16\mu\tau^2} \cdot t, \quad (2)$$

with h resin capillary rise height, F_{geo} geometric factor, D_h equivalent hydraulic diameter, γ surface tension of the fluid, θ contact angle between resin and fibre, μ fluid dynamic viscosity, τ tortuosity of the VACNTs, and t VACNTs-resin contact time.

While the equivalent diameter can be calculated as

$$D_h = \frac{d_{VACNTs} (1 - \psi_{VACNTs})}{\psi_{VACNTs}}, \quad (3)$$

with D_h equivalent diameter, d_{VACNTs} VACNTs' average diameter, and ψ_{VACNTs} VACNTs' volume fraction.

The surface tension of the prepreg resin, the contact angle, the tortuosity, and the geometric factor can be challenging to determine due to the nanoscale size of individual nanotubes. However, these parameters could be assumed as a constant C to study the effects of time and resin capillary rise height. LW equation [Eq. (2)] can then be formulated as

$$h = C \sqrt{\frac{t}{\mu}}, \quad (4)$$

with C empirical coefficient that can be found by experimental results, t VACNTs-resin contact time, and μ fluid dynamic viscosity.

Figure 4 summarises the measurements of capillary rise height over time in the VACNTs based on the SEM observations. Two values of temperature (60 °C and 80 °C) correspond to 280 Pa.s and 60 Pa.s of resin viscosity, respectively.

Based on the measured capillary rise at 60 °C, the constant C can be identified to draw a regression curve at both 60 °C and 80 °C with known values of resin viscosity. It can be observed that the capillary rise height progresses gradually in the targeted interval of time, from 0 to 20 min. Therefore, even in case of dense VACNTs' forests (2×10^{11} nanotubes/cm²), resin partial capillary rise height can be controlled when resin viscosity value is in the vicinity of 280 Pa.s. Constituent material properties, such as prepreg surface roughness, VACNTs' tortuosity, and VACNTs' limited height, could be the main factors which exacerbate the deviation in resin capillary height determination.

When heating the resin to 80 °C, due to low resin viscosity, uncontrolled capillary rise has occurred and resin from prepreg has completely impregnated VACNTs' forests upon 5 min, as shown in Fig. 3b. This observation is consistent with theoretical curve in Fig. 4, which shows that resin would reach 30 μ m of height in less than 6 min. Therefore,

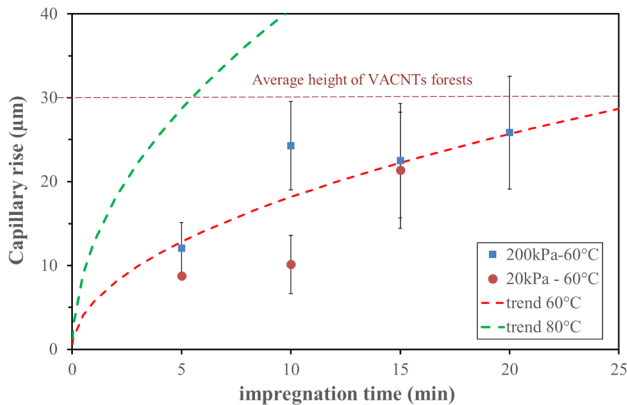


Fig. 4 Resin capillary rise curve (h-t relation)

the experimental results in capillary rise height cannot be reported in 80 °C heating in our study.

2.5 Buckling of VACNTs

Both the LW model and the experimental measurements show no effect of the contact pressure. However, while carbon nanotubes demonstrate tremendous tensile properties, long and slender nanotubes can be prone to buckling when subjected to longitudinal compression. At microscopic scale, the unidirectional prepreg surface can also demonstrate a certain level of roughness. While increasing the applied pressure can improve the contact between the prepreg and the VACNTs' forest, care must be taken not to damage the vertical alignment of the carbon nanotubes. Figure 5 presents observations of VACNTs transferred on the prepreg after capillary impregnation at two levels of compaction. Both were impregnated at 60 °C with a contact duration of 5 min. On Fig. 5a, the applied pressure was 20 kPa, and the VACNTs remain straight and vertically aligned. On Fig. 5b, after compaction at 200 kPa, some buckling can be observed on the VACNTs' forest. While the buckling remains minimal, this demonstrates the limit to ensure proper vertical alignment of the nanotubes.

3 Conclusion

The feasibility and control of capillary impregnation of VACNTs' forest using the resin of the prepreg have been demonstrated, and a few preconisations can be made.

The characterisation of the height and density of VACNTs' forests is necessary to calculate the quantity of resin needed for impregnation. The chosen prepreg needs to have sufficient resin flow to ensure good impregnation.

The capillary impregnation of the resin into the VACNTs can be controlled by careful selection of temperature and contact time. A partial impregnation is more favourable to ensure efficient transfer of VACNTs from their growth substrate to the prepreg. The capillary impregnation in the VACNTs follows the Lucas-Washburn model with impregnation height increasing as a function of $t^{1/2}$. Although a temperature of 80 °C was not favourable in this study, due to the chosen minimal time and the experimental apparatus used, faster heating and cooling rates could allow efficient impregnation and subsequent transfer at higher temperature.

The contact pressure applied between the VACNTs and prepreg does not significantly impact the speed of capillary impregnation. While sufficient pressure is needed to ensure a uniform and intimate contact between the prepreg and the VACNTs' forests, the applied pressure should not exceed the buckling stress of the VACNTs' forest.

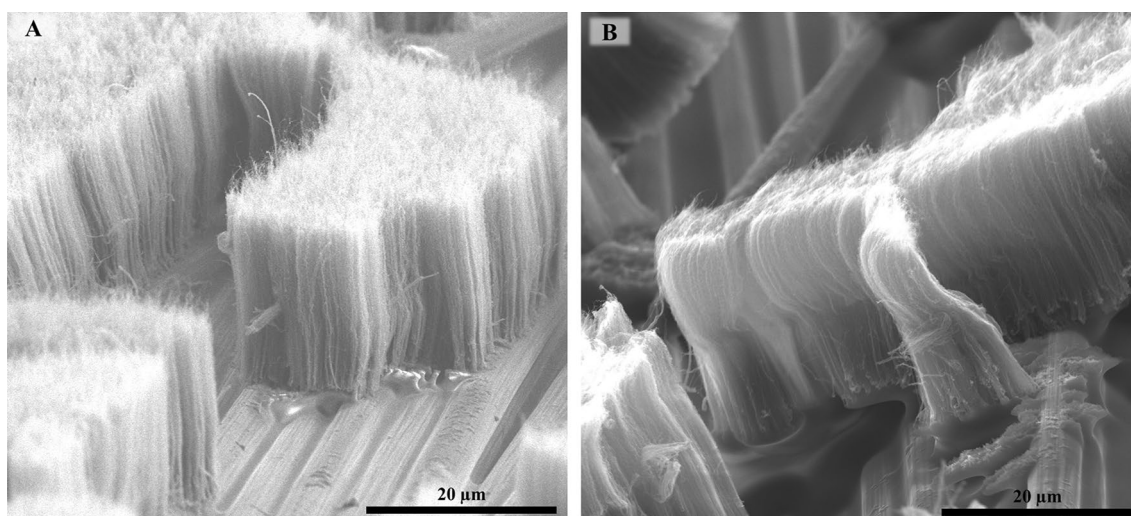


Fig. 5 VACNTs' forests transferred onto prepreg at: **a** 20 kPa pressure and **b** 200 kPa pressure

The feasibility of nano-structured hybrid composite impregnation aims to determine the range of process parameters. These factors are key to study the scalability of VACNTs-prepreg transfer. Mechanical characterisations of this novel material will be investigated afterwards.

Acknowledgements This work was carried out within the framework of the FUI ATIHS project (improving satellite structures strength against hypervelocity impacts from space debris) funded by Bpifrance and Région Occitanie. The authors also thank the partners of the ATIHS project (DynaS+, Thiot Ingenierie, CEA Saclay, CEA Cesta, NAWATechnologies, Armines, and Airbus Defence&Space) for the fruitful exchanges carried out in this context. Special thanks are due to Alexandre Sangar (NAWATechnologies) for helpful discussions and instructions on the TIMA apparatus, and to Karine Vieilleveigne for performing the SEM observations.

Data availability The datasets analysed during the current study are available from the corresponding author on reasonable request.

Declarations

Conflict of interest The authors have no relevant financial or non-financial interests to disclose.

References

1. Rubino F, Nisticò A, Tucci F, Carlone P (2020) Marine application of fiber reinforced composites: a review. *J Mar Sci Eng* 8:26. <https://doi.org/10.3390/jmse8010026>
2. Pendhari SS, Kant T, Desai YM (2008) Application of polymer composites in civil construction: a general review. *Compos Struct* 84:114–124. <https://doi.org/10.1016/j.compstruct.2007.06.007>
3. Liu Y, Du H, Liu L, Leng J. Shape memory polymers and their composites in aerospace applications: a review. *Smart Mater Struct* 2014;23:023001. <https://doi.org/10.1088/0964-1726/23/2/023001>.
4. Kausar A, Rafique I, Muhammad B (2016) Review of Applications of polymer/carbon nanotubes and Epoxy/CNT composites.

Polym-Plast Technol Eng 55:1167–1191. <https://doi.org/10.1080/03602559.2016.1163588>

5. Nettles A, Hodge A, Jackson J (2011) An examination of the compressive cyclic loading aspects of damage tolerance for polymer matrix launch vehicle hardware. *J Compos Mater* 45:437–458. <https://doi.org/10.1177/0021998310376117>
6. Sørensen BF. 11 - Delamination fractures in composite materials. In: Talreja R, Varna J, editors. *Model. Damage Fatigue Fail. Compos. Mater.*, Woodhead Publishing; 2016, p. 213–40. <https://doi.org/10.1016/B978-1-78242-286-0.00011-X>.
7. Dransfield K, Baillie C, Mai Y-W (1994) Improving the delamination resistance of CFRP by stitching—a review. *Compos Sci Technol* 50:305–317. [https://doi.org/10.1016/0266-3538\(94\)90019-1](https://doi.org/10.1016/0266-3538(94)90019-1)
8. Nouruzi N, Dinari M, Gholipour B, Afshari M, Rostamnia S (2022) In situ organized pd and au nanoparticles in a naphthalene-based imine-linked covalent triazine framework for catalytic suzuki reactions and H₂ generation from formic acid. *ACS Appl Nano Mater* 5:6241–6248. <https://doi.org/10.1021/acsanm.2c00285>
9. Mohtasham H, Gholipour B, Rostamnia S, Ghiasi-Moaser A, Farajzadeh M, Nouruzi N, et al. Hydrothermally exfoliated P-doped g-C₃N₄ decorated with gold nanorods for highly efficient reduction of 4-nitrophenol. *Colloids Surf Physicochem Eng Asp* 2021;614:126187. <https://doi.org/10.1016/j.colsurfa.2021.126187>.
10. Doustkhah E, Mohtasham H, Farajzadeh M, Rostamnia S, Wang Y, Arandiyani H, et al. Organosiloxane tunability in mesoporous organosilica and punctuated Pd nanoparticles growth; theory and experiment. *Microporous Mesoporous Mater* 2020;293:109832. <https://doi.org/10.1016/j.micromeso.2019.109832>.
11. Karimi-Maleh H, Alizadeh M, Orooji Y, Karimi F, Baghayeri M, Rouhi J et al (2021) Guanine-based DNA biosensor amplified with Pt/SWCNTs nanocomposite as analytical tool for nanomolar determination of daunorubicin as an anticancer drug: a docking/experimental investigation. *Ind Eng Chem Res* 60:816–823. <https://doi.org/10.1021/acs.iecr.0c04698>
12. Sabaghnia N, Janmohammadi M, Dalili M, Karimi Z, Rostamnia S (2019) Euphorbia leaf extract-assisted sustainable synthesis of Au NPs supported on exfoliated GO for superior activity on water purification: reduction of 4-NP and MB. *Environ Sci Pollut Res* 26:11719–11729. <https://doi.org/10.1007/s11356-019-04437-2>
13. Domun N, Hadavinia H, Zhang T, Sainsbury T, Liaghat GH, Vahid S (2015) Improving the fracture toughness and the strength

- of epoxy using nanomaterials—a review of the current status. *Nanoscale* 7:10294–10329. <https://doi.org/10.1039/C5NR01354B>
14. Nam TH, Goto K, Kamei T, Shimamura Y, Inoue Y, Kobayashi S et al (2019) Improved mechanical properties of aligned multi-walled carbon nanotube/thermoplastic polyimide composites by hot stretching. *J Compos Mater* 53:1241–1253. <https://doi.org/10.1177/0021998318796916>
 15. Tong X, Liu C, Cheng H-M, Zhao H, Yang F, Zhang X (2004) Surface modification of single-walled carbon nanotubes with polyethylene via in situ Ziegler-Natta polymerization. *J Appl Polym Sci* 92:3697–3700. <https://doi.org/10.1002/app.20306>
 16. Jia Z, Wang Z, Xu C, Liang J, Wei B, Wu D et al (1999) Study on poly(methyl methacrylate)/carbon nanotube composites. *Mater Sci Eng A* 271:395–400. [https://doi.org/10.1016/S0921-5093\(99\)00263-4](https://doi.org/10.1016/S0921-5093(99)00263-4)
 17. Mezdour D, Tabellout M, Bouanga CV, Sahli S. Electrical properties of polyamide/polyaniline composite films. *J Phys Conf Ser* 2009;183:012017. <https://doi.org/10.1088/1742-6596/183/1/012017>.
 18. Sandler J, Shaffer MSP, Prasse T, Bauhofer W, Schulte K, Windle AH (1999) Development of a dispersion process for carbon nanotubes in an epoxy matrix and the resulting electrical properties. *Polymer* 40:5967–5971. [https://doi.org/10.1016/S0032-3861\(99\)00166-4](https://doi.org/10.1016/S0032-3861(99)00166-4)
 19. Dong Z, Sun B, Zhu H, Yuan G, Li B, Guo J et al (2021) A review of aligned carbon nanotube arrays and carbon/carbon composites: fabrication, thermal conduction properties and applications in thermal management. *New Carbon Mater* 36:873–892. [https://doi.org/10.1016/S1872-5805\(21\)60090-2](https://doi.org/10.1016/S1872-5805(21)60090-2)
 20. Kaur S, Ravavikar N, Helms BA, Prasher R, Ogletree DF (2014) Enhanced thermal transport at covalently functionalized carbon nanotube array interfaces. *Nat Commun* 5:3082. <https://doi.org/10.1038/ncomms4082>
 21. Peacock MA, Roy CK, Hamilton MC, Wayne Johnson R, Knight RW, Harris DK (2016) Characterization of transferred vertically aligned carbon nanotubes arrays as thermal interface materials. *Int J Heat Mass Transf* 97:94–100. <https://doi.org/10.1016/j.ijheatmasstransfer.2016.01.071>
 22. Tong T, Zhao Y, Delzeit L, Kashani A, Meyyappan M, Majumdar A (2007) Dense vertically aligned multiwalled carbon nanotube arrays as thermal interface materials. *IEEE Trans Compon Packag Technol* 30:92–100. <https://doi.org/10.1109/TCAPT.2007.892079>
 23. Zhu J, Kim J, Peng H, Margrave JL, Khabashesku VN, Barrera EV (2003) Improving the dispersion and integration of single-walled carbon nanotubes in epoxy composites through functionalization. *Nano Lett* 3:1107–1113. <https://doi.org/10.1021/nl0342489>
 24. Zhang X-H, Zhang Z-H, Xu W-J, Chen F-C, Deng J-R, Deng X (2008) Toughening of cycloaliphatic epoxy resin by multiwalled carbon nanotubes. *J Appl Polym Sci* 110:1351–1357. <https://doi.org/10.1002/app.28590>
 25. Zhu J, Peng H, Rodriguez-Macias F, Margrave JL, Khabashesku VN, Imam AM et al (2004) Reinforcing epoxy polymer composites through covalent integration of functionalized nanotubes. *Adv Funct Mater* 14:643–648. <https://doi.org/10.1002/adfm.200305162>
 26. Garcia EJ, Wardle BL, John HA (2008) Joining prepreg composite interfaces with aligned carbon nanotubes. *Compos Part Appl Sci Manuf* 39:1065–1070. <https://doi.org/10.1016/j.compositesa.2008.03.011>
 27. Wardle BL, Kim S-G. Nano-engineered material architectures: Ultra-tough hybrid nanocomposite system, 2009.
 28. Garcia EJ, Hart AJ, Wardle BL, Slocum AH. Fabrication of composite microstructures by capillarity-driven wetting of aligned carbon nanotubes with polymers. *Nanotechnology* 2007;18:165602. <https://doi.org/10.1088/0957-4484/18/16/165602>.
 29. Beard JD, Rouholamin D, Farmer BL, Evans KE, Ghita OR (2015) Control and modelling of capillary flow of epoxy resin in aligned carbon nanotube forests. *RSC Adv* 5:39433–39441. <https://doi.org/10.1039/C5RA03393D>
 30. Sojoudi H, Kim S, Zhao H, Annavarapu RK, Mariappan D, Hart AJ et al (2017) Stable wettability control of nanoporous microstructures by iCVD coating of carbon nanotubes. *ACS Appl Mater Interfaces* 9:43287–43299. <https://doi.org/10.1021/acsami.7b13713>
 31. Bergonzo P, Tromson D, Mer C (2006) CVD diamond-based semi-transparent beam-position monitors for synchrotron beamlines: preliminary studies and device developments at CEA/Saclay. *J Synchrotron Radiat* 13:151–158. <https://doi.org/10.1107/S0909049505032097>
 32. Mayne-L’Hermite M, Pinault M, Mierczynska A, Barrau S, Pichot V, Khodja H, et al. Nanotubes de carbone alignés synthétisés par CVD d’aérosol : mécanismes de croissance et applications 2006:8.
 33. TIMA. Nanotest Homepage 2018. <https://www.nanotest.eu/en/tima/> (accessed October 23, 2018).
 34. Washburn EW (1921) The dynamics of capillary flow. *Phys Rev* 17:273–283. <https://doi.org/10.1103/PhysRev.17.273>
 35. Ahn KJ, Seferis JC, Berg JC (1991) Simultaneous measurements of permeability and capillary pressure of thermosetting matrices in woven fabric reinforcements. *Polym Compos* 12:146–152. <https://doi.org/10.1002/pc.750120303>
 36. LeBel F, Fanaei AE, Ruiz É, Trochu F (2012) Experimental characterization by fluorescence of capillary flows in the fiber tows of engineering fabrics. *Open J Inorg Non-Met Mater* 2:25–45. <https://doi.org/10.4236/ojinm.2012.23004>